

RESEARCH ARTICLE | APRIL 03 2023

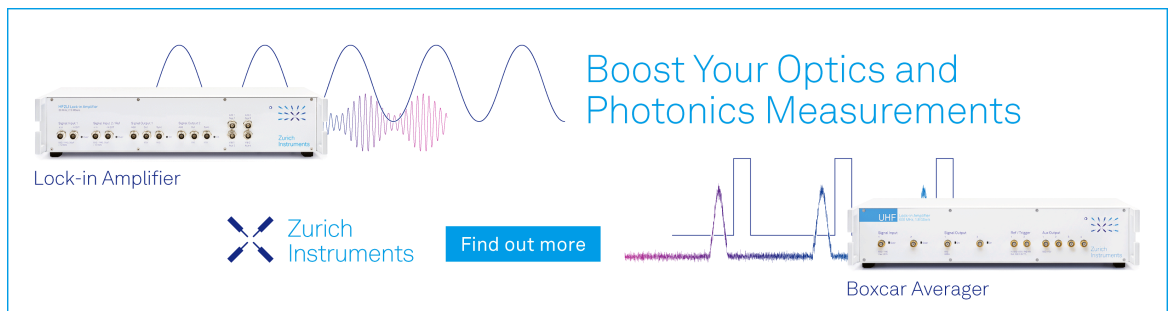
Molecular modeling and simulation of aqueous solutions of alkali nitrates

Dominik Schaefer ; Maximilian Kohns  ; Hans Hasse 



J. Chem. Phys. 158, 134508 (2023)

<https://doi.org/10.1063/5.0141331>



Boost Your Optics and Photonics Measurements

Lock-in Amplifier

Zurich Instruments

Find out more

Boxcar Averager

Molecular modeling and simulation of aqueous solutions of alkali nitrates

Cite as: J. Chem. Phys. 158, 134508 (2023); doi: 10.1063/5.0141331

Submitted: 5 January 2023 • Accepted: 13 March 2023 •

Published Online: 3 April 2023



View Online



Export Citation



CrossMark

Dominik Schaefer,  Maximilian Kohns,^{a)}  and Hans Hasse 

AFFILIATIONS

Laboratory of Engineering Thermodynamics (LTD), RPTU Kaiserslautern, 67663 Kaiserslautern, Germany

^{a)} Author to whom correspondence should be addressed: maximilian.kohns@mv.uni-kl.de

ABSTRACT

A set of molecular models for the alkali nitrates (LiNO_3 , NaNO_3 , KNO_3 , RbNO_3 , and CsNO_3) in aqueous solutions is presented and used for predicting the thermophysical properties of these solutions with molecular dynamics simulations. The set of models is obtained from a combination of a model for the nitrate anion from the literature with a set of models for the alkali cations developed in previous works of our group. The water model is SPC/E and the Lorentz–Berthelot combining rules are used for describing the unlike interactions. This combination is shown to yield fair predictions of thermophysical and structural properties of the studied aqueous solutions, namely the density, the water activity and the mean ionic activity coefficient, the self-diffusion coefficients of the ions, and radial distribution functions, which were studied at 298 K and 1 bar; except for the density of the solutions of all five nitrates and the activity properties of solutions of NaNO_3 , which were also studied at 333 K. For calculating the water the activity and the mean ionic activity coefficient, the OPAS (*osmotic pressure for the activity of solvents*) method was applied. The new models extend an ion model family for the alkali halides developed in previous works of our group in a consistent way.

© 2023 Author(s). All article content, except where otherwise noted, is licensed under a Creative Commons Attribution (CC BY) license (<http://creativecommons.org/licenses/by/4.0/>). <https://doi.org/10.1063/5.0141331>

I. INTRODUCTION

Thermophysical properties of electrolyte solutions are difficult to model due to the strong electrostatic interactions between the ions as well as the strong interaction between the ions and the solvent molecules. Models of the excess Gibbs energy, such as the Pitzer model¹ and its extensions^{2–5} or the electrolyte–NRTL⁶ model, build on the Debye and Hückel⁷ theory but require the adjustment of many parameters and are, thus, mainly used as correlation tools. Also equations of state for electrolytes have been developed, such as ePC-SAFT,^{8,9} eCPA,^{10,11} and SAFT- γ Mie,^{12,13} which, in contrast to the models of the excess Gibbs energy mentioned above, also describe volumetric properties but still do not give access to structural and transport properties. Molecular modeling and simulation based on force fields is a viable route for describing electrolyte solutions. Molecular models are built on a strong physical background and hence enable robust extrapolations with comparatively few adjustable parameters. Furthermore, they basically yield all thermodynamic and transport properties as well as information on structural properties. The state of research on molecular modeling and simulation of electrolyte solutions has recently been reviewed

by Smith *et al.*¹⁴ and Panagiotopoulos.¹⁵ In the present work, we use this approach for predicting the properties of alkali nitrates in an aqueous solution. The molecular models we combine have not been trained to data of these solutions and they stem from different groups. Hence, this work can also be understood as a study of the predictive power of molecular models of electrolyte solutions.

In a previous study of our group,^{16,17} we have developed a set of molecular models for the alkali halide salts in an aqueous solution. All models of this set consist of a single Lennard–Jones (LJ) interaction site with a superimposed point charge and are non-polarizable. The alkali halide models were adjusted to the thermophysical and structural properties of the aqueous solution in conjunction with the SPC/E water model.¹⁸ For the alkali and halide ion models, the length parameter σ of the LJ potential was adjusted to the density of the solution at 293.15 K¹⁶, and the energy parameter ϵ has been adjusted to the self-diffusion coefficients and radial distribution functions (RDF) at 293.15–298.15 K.¹⁷ In the present work, we wanted to extend this model family by a more complex ion model. Due its high practical relevance, we have chosen the nitrate anion, i.e., the aim is to add LiNO_3 , NaNO_3 , KNO_3 , RbNO_3 , and CsNO_3 to the set. Aqueous solutions of nitrate salts are found in nature

as well as in many industrial processes. Examples include the production of fertilizers, nutrition, pharmaceuticals, glass, enamel, and explosives.¹⁹

There is a wide range of water models in the literature, e.g., the TIP4P,²⁰ SPC,²¹ SPC/E,¹⁸ or OPC²² models. These models yield fair descriptions of thermophysical properties such as density and dielectric constant, and structural properties at near-ambient conditions. As a water model for the alkali nitrate model set, we chose the SPC/E water model, since alkali cation model parameters were adjusted in conjunction with the SPC/E water model, which leaves us with the choice of the nitrate model.

Different types of molecular models have been used in the literature for describing the nitrate ion. We focus here on rigid, non-polarizable models based on a combination of LJ and point charge interaction sites, as this is consistent with the alkali ion models. Three models of that class have been proposed in the literature: Vchirawongkwin *et al.*,^{23–27} Laaksonen and Kovacs,^{28,29} and Krienke and Schmeer.^{30–33} Alternative approaches include flexible models^{34,35} and models in which the basic sites are polarizable^{36–39} or hard-spheres.^{40,41} Combining different ion models that were developed in conjunction with the same water model seems to be a reasonable approach, but this does not guarantee fair predictions and was not possible in the case of these three models: The models by Vchirawongkwin *et al.*, Laaksonen, and Kovacs were developed and tested in combination with the SPC²¹ model, while the model by Krienke and Schmeer was first used in combination with a tailored water model of the authors and has found no wider applications. We first expected that the nitrate models from the literature would serve only as a starting point for a further optimization. However, preliminary tests showed that the nitrate model of Krienke and Schmeer³⁰ predicted the density of aqueous solutions of alkali nitrates as a function of molality most reliable in conjunction with the set of alkali ions from our previous work^{16,17} and the SPC/E water model, without any adjustments. The other two nitrate models overestimated the solution density by far when applied in the same way. Hence, we have decided to use the nitrate model of Krienke and Schmeer in the new model set for alkali nitrates without any modifications.

Krienke and Schmeer³⁰ adopted the LJ parameters of a hybrid quantum–classical nitrate model of Lebrero *et al.*,⁴² where the hybrid quantum–classical nitrate model was used in conjunction with the TIP4P²⁰ and TIP4P-FQ⁴³ water models. Krienke and Schmeer³⁰ derived the distances between the nitrogen and the oxygen interaction sites by an *ab initio* approximation of the second order Møller–Plesset perturbation theory (MP2/6-31G(d)) and the partial charges of each interaction site by a Mulliken population analysis. The new nitrate model was used in combination with a tailored water model in Monte Carlo simulations to investigate the hydration of anions with oxygen sites.³⁰ The nitrate model of Krienke and Schmeer has also been used in conjunction with the SPC/E¹⁸ water model and different cation models from the literature to investigate the hydration,^{30,31} structure,³² and the self-diffusion and electric conductivity³³ of nitrate salts in aqueous solutions.

As all models were adopted from the literature and no adjustments were made (the cross interactions were determined from the Lorentz–Berthelot combining rules), all results are predictions. The work can also be considered as a case study for the possibility to

combine ion models (of different authors) in a building-block like manner. A broad range of properties were studied: the density, the water activity and the mean ionic activity coefficient, the self-diffusion coefficient, and radial distribution functions. The temperature and pressure were always 298.15 K, 1 bar, with the exception of the density (for all studied nitrate salts) and the water activity, and the mean ionic activity coefficient (for NaNO₃), which were additionally investigated at 333.15 K.

The sampling of entropic properties in molecular dynamics (MD) is a demanding task. Different approaches have been developed in recent years for sampling such properties.^{44–49} In this work, water activity and related properties, such as the osmotic pressure and the mean ionic activity coefficients, were determined by the OPAS (*osmotic pressure for the activity of solvents*) method.^{50–52}

II. MOLECULAR MODELING AND SIMULATION

A. Molecular models

All investigated molecular models in this work have two types of interaction sites: Lennard-Jones sites (LJ) and point charge sites (C). The potential energy u_{ij} of the interaction of two particles i and j is, hence, given by

$$u_{ij} = u_{ij}^{\text{LJ}} + u_{ij}^{\text{C}} = \sum_{a=1}^{N_i^{\text{LJ}}} \sum_{b=1}^{N_j^{\text{LJ}}} 4\epsilon_{ijab} \left[\left(\frac{\sigma_{ijab}}{r_{ijab}} \right)^{12} - \left(\frac{\sigma_{ijab}}{r_{ijab}} \right)^6 \right] + \sum_{c=1}^{N_i^{\text{C}}} \sum_{d=1}^{N_j^{\text{C}}} \frac{1}{4\pi\epsilon_0} \frac{q_{ic}q_{jd}}{r_{ijcd}}, \quad (1)$$

where N_i is the total number of interaction sites of either type on particle i , $a-d$ are indices for the respective interaction sites, r_{ijab} denotes the distance between the interaction site a on particle i and the interaction site b on particle j , and ϵ_{ijab} and σ_{ijab} are the energy and size parameter of the LJ potential. q_{ic} and q_{jd} are the magnitude of the point charge, and ϵ_0 is the vacuum permittivity. Unlike LJ interactions are modeled with the Lorentz–Berthelot rules,^{53,54}

$$\sigma_{ijab} = \frac{\sigma_{ia} + \sigma_{jb}}{2}, \quad (2)$$

$$\epsilon_{ijab} = \sqrt{\epsilon_{ia}\epsilon_{jb}}. \quad (3)$$

Figure 1 shows a representation of the molecular model of the nitrate anion that was used in the present work, which was taken from Krienke and Schmeer,³⁰ and the corresponding Lewis formula. The model is planar, rigid, and non-polarizable and consists of one central nitrogen (N) and three identical oxygen (O_N) interaction sites. Each of the interaction sites comprises a LJ site and a point charge that is superimposed in the center of the LJ site. The O_N sites are positioned on an equilateral triangle, with the N in its center. The bond length is $r_{\text{N-O}_N} = 1.27$ Å. All three O_N sites have the same LJ parameters and negative point charge, while the parameters of the N site are different. All four point charges sum up to a net charge of $-1 e$.

The nitrate model was used together with a set of alkali^{16,17} ion models developed in previous work of our group. All cation models consist of a single LJ site with a superimposed point charge of $+1 e$

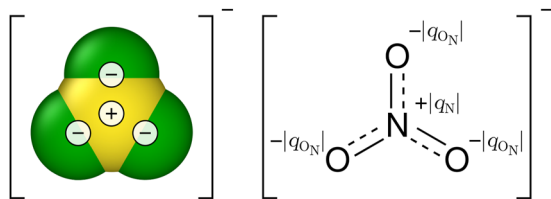


FIG. 1. The nitrate anion: depiction of the molecular model used in the present work (left panel) and Lewis formula (right panel). The + and – signs in the left panel represent the point charges on the nitrogen (N, yellow) and oxygen (O_N , green) that are placed on the center of the corresponding LJ interaction sites. The model is planar. The dashed lines between nitrogen and oxygen in the Lewis formula represent mesomeric bonds.

in its center. We consider the five alkali cations Li^+ , Na^+ , K^+ , Rb^+ , and Cs^+ .

Throughout this work, the SPC/E water model¹⁸ was employed, since cation models were developed for use together with this water model.¹⁷ The SPC/E water model consists of a single LJ site (O_W) and three partial charges, one of which is placed on the center of O_W , while the other two are located a distance of 1 Å apart from the central O_W site and form a bond angle of 109.47° with O_W .

The parameters of all molecular models employed in this work are compiled in Table I.

B. Studied thermophysical and structural properties

1. Reduced density

An essential thermophysical property of electrolyte solutions is their density. Here, we focused on the concentration dependence, i.e., the effect of adding nitrate salts to water at constant temperature and pressure. To characterize the amount of salt, we use the overall molality \tilde{b}_{AB} of the salt AB, which is defined as

$$\tilde{b}_{AB} = \frac{\tilde{n}_{AB}}{m_W}, \quad (4)$$

where \tilde{n}_{AB} is the overall mole number of salt AB in the solution (disregarding the dissociation) and m_W the mass of pure water in the

TABLE I. Summary of the parameters of the molecular models used in this work. The nitrate model is rigid and flat, the angle between the N and the O_N sites is 120° , the distance between these sites is $r = 1.27$ Å. For the SPC/E water model, the angle between the O_W and the H sites is 109.47° and the distance between H sites and the O_W is $r = 1$ Å.

Species	Site	$\sigma/\text{\AA}$	$\epsilon/k_B/\text{K}$	q/e	Reference
Nitrate	N	3.9	100.716	+0.8603	30
	O_N	3.154	78.057	-0.6201	
	Li^+	1.88	200	+1	
	Na^+	1.89			
Alkaline cations	K^+	2.77			17
	Rb^+	3.26			
	Cs^+	3.58			
	O_W	3.166	78.198	-0.8476	
Water	H			+0.4238	18

solution. The overall molality depends linearly on the amount of salt in the solution in contrast to the mole fraction. Following our previous work,^{16,17,55} instead of studying the absolute value of the density ρ , we study the reduced density ρ^* , which is defined as

$$\rho^*(T, p, \tilde{b}_{AB}) = \frac{\rho^{(m)}(T, p, \tilde{b}_{AB})}{\rho_W^{(m)}(T, p)}, \quad (5)$$

where the density of the solution $\rho^{(m)}$ is divided by the density of pure water $\rho_W^{(m)}$. This definition sets the focus on the concentration dependence and eliminates the influence of the quality of the description of the density of pure water by the water model. It has been found for many salts that the density of the solution increases almost linearly as a function of the overall molality up to quite high salt molalities.^{16,56,57} The density of pure SPC/E water as determined in molecular simulations under the usage of the Ewald summation as a long range correction from the present work is compared with experimental literature data in Table II confirming the good quality of the description.

For comparison with the present simulation data, experimental data on the density of aqueous alkali nitrate solutions at 298 K and near ambient pressure were taken from the Dortmund Data Bank⁵⁹ and correlated as a function $\rho^*(\tilde{b}_{AB})$ using a second order polynomial of the form,

$$\rho^*(\tilde{b}_{AB}) = 1 + \alpha_{AB,1} \tilde{b}_{AB} + \alpha_{AB,2} \tilde{b}_{AB}^2, \quad (6)$$

where $\alpha_{AB,1}$ and $\alpha_{AB,2}$ are adjustable parameters. The polynomial is only used as a reference for the simulation data of this work to the experimental data from the literature. More information on the fitting procedure to the experimental density data and the handling of outliers is given in the supplementary material, where also the values of $\alpha_{AB,1}$ and $\alpha_{AB,2}$ for each nitrate salt considered in this work are reported.

2. Water activity and mean ionic activity coefficient

The overall chemical potential $\tilde{\mu}_{AB}$ of a salt AB that dissociates into the cation A^+ and the anion B^- in an electrolyte solution is normalized as shown in Eq. (7):

$$\tilde{\mu}_{AB}(T, p, \underline{x}) = \tilde{\mu}_{AB}^{\text{ref}b}(T, p, \underline{x}^*) + RT \ln \left(\frac{\tilde{b}_{AB}}{b^0} \tilde{\gamma}_{AB}^{b*}(T, p, \underline{x}) \right). \quad (7)$$

Herein, $\tilde{\mu}_{AB}^{\text{ref}b}$ is the overall chemical potential of the electrolyte in the reference state, \tilde{b}_{AB} is the overall molality of the salt AB, and b^0 is set to 1 mol kg^{-1} . The vectors \underline{x} and \underline{x}^* characterize the composition of the studied mixtures and the mixture in the reference state,

TABLE II. Density of pure water determined in this work for the SPC/E water model and experimental data from the literature⁵⁸ at different temperatures. The values shown here are used as reference for the reduced density, cf. Eq. (5). Statistical uncertainties are given in parentheses.

T/K	$\rho_W^{\text{sim.}}/\text{kg m}^{-3}$	$\rho_W^{\text{Expt.}}/\text{kg m}^{-3}$
298.15	1004.3(1)	997.05
333.15	982.9(1)	983.20

respectively. Furthermore, γ_{AB}^{b*} is the mean ionic activity coefficient of the salt AB, which is defined as

$$\gamma_{AB}^{b*}(T, p, \underline{x}) = \left[\left(\gamma_{A^+}^{b*}(T, p, \underline{x}) \right)^{v_{A^+}} \left(\gamma_{B^-}^{b*}(T, p, \underline{x}) \right)^{v_{B^-}} \right]^{1/(v_{A^+} + v_{B^-})}, \quad (8)$$

where $\gamma_{A^+}^{b*}$ and $\gamma_{B^-}^{b*}$ as well as v_{A^+} and v_{B^-} are the activity coefficients and the stoichiometric coefficients of the cation A^+ and the anion B^- , respectively. The activity coefficients go to 1 for infinite dilution of the salt.

The water activity a_W , on the other hand, is normalized according to Raoult's law as

$$\tilde{\mu}_W(T, p, \underline{x}) = \tilde{\mu}_W^{\text{ref}}(T, p) + RT \ln(a_W(T, p, \underline{x})). \quad (9)$$

Herein, the reference state is the pure liquid solvent water at the studied T and p .

The water activity a_W is directly related to the osmotic pressure Π as shown in Eq. (10),

$$\ln(a_W) = -\frac{\Pi}{\rho_W^{(n)} RT}, \quad (10)$$

where $\rho_W^{(n)}$ is the molar density of the pure solvent, T is the temperature, and R is the universal gas constant. The osmotic pressure was determined in this work by the OPAS method. The water activity a_W as a function of overall molality \tilde{b}_{AB} of an 1:1 electrolyte was correlated by^{45,51,60}

$$\begin{aligned} \ln(a_W) = & -2M_W(\tilde{b}_{AB}/b^0) - M_W \ln(10) \left(\beta(\tilde{b}_{AB}/b^0)^2 \right. \\ & + \frac{3}{4}C(\tilde{b}_{AB}/b^0)^3 + \frac{2A}{B^3 + B^4\sqrt{\tilde{b}_{AB}/b^0}} \\ & \left. + \frac{4A \ln(B\sqrt{\tilde{b}_{AB}/b^0} + 1)}{B^3} - \frac{2A\sqrt{\tilde{b}_{AB}/b^0}}{B^2} - \frac{2A}{B^3} \right), \quad (11) \end{aligned}$$

where B , β , and C are adjustable parameters. The parameter A stems from Debye-Hückel theory^{48,50,60} and is

$$A = \frac{e^3 \sqrt{2\rho_W^{(m)} N_{\text{avo}}}}{(4\epsilon_0 \epsilon_r k_B T)^{3/2}} \frac{1}{\pi \ln(10)}, \quad (12)$$

where ϵ_r is the relative permittivity of the pure solvent, k_B is the Boltzmann constant, $\rho_W^{(m)}$ is the mass density of pure water, and N_{avo} is the Avogadro number. In this work, for SPC/E water we use $\epsilon_r(298 \text{ K}) = 71$,⁶¹ $\epsilon_r(333 \text{ K}) = 62.1$,⁶² and the densities $\rho_W^{(m)}$ from Table II, which results in $A(298 \text{ K}) = 0.5938$ and $A(333 \text{ K}) = 0.608$. The correlation shown in Eq. (11) can be used to calculate the mean ionic activity coefficient γ_{AB}^{b*} as a function of the overall molality \tilde{b}_{AB} with

$$\ln \gamma_{AB}^{b*} = \ln(10) \left(\frac{-A\sqrt{\tilde{b}_{AB}/b^0}}{1 + B\sqrt{\tilde{b}_{AB}/b^0}} + \beta(\tilde{b}_{AB}/b^0) + C(\tilde{b}_{AB}/b^0)^2 \right). \quad (13)$$

3. Self-diffusion coefficient

The self-diffusion coefficient D_i is a measure for the Brownian movement of a single particle of the type i in a fluid in equilibrium. In this work, D_i was determined using the Green-Kubo formalism,^{63–65}

$$D_i = \frac{1}{3N_i} \int_0^\infty \langle v_{k,i}(\tau=0) \cdot v_{k,i}(\tau) \rangle d\tau, \quad (14)$$

where N_i is the total number of particles of component i , $v_{k,i}(\tau)$ is the velocity of a particle k of component i at time τ , and the angular brackets denote the ensemble average.

4. Radial distribution function

The radial distribution function $g_{i-j}(r)$ of particles of type j around particles of type i was used for quantifying the structure of the studied electrolyte solutions. It is defined as⁶⁶

$$g_{i-j}(r) = \frac{1}{\rho_j^{(n)}} \frac{dN_j}{4\pi r^2 dr}, \quad (15)$$

where r is the distance between the center of particle i (for the nitrate ion, the center of the O_N or the N site) and an infinitesimally thin shell with a thickness dr , dN_j is the number of particles of component j inside this shell, and $\rho_j^{(n)}$ is the number density of particles of component j in the bulk.

C. Simulation details

All simulations of this work were molecular dynamics (MD) simulations and were carried out with the program *ms2*.⁶¹ The number of particles was 4000 except for the simulations of self-diffusion coefficients, where it was 16 000, as highly diluted mixtures were studied. The simulation volume was cubic and periodic boundary conditions were applied in all directions. Particle positions were initialized randomly on a cubic grid. The equations of motion were integrated with a fifth order Gear predictor corrector algorithm,^{66,67} using a time step of 1.214 fs. A cut-off radius of 15 Å was used for all interactions. Standard tail corrections were applied for the LJ interactions.⁶⁶ Ewald summation⁶⁸ was applied for the long-range electrostatics, considering up to 10 k -vectors in each Cartesian direction, using the real space convergence parameter $\kappa = 5.6$, and conducting boundary conditions. The temperature was controlled using the velocity scaling thermostat.⁶⁶ The statistical uncertainties of the simulation results were estimated with the blocking method described by Flyvbjerg and Petersen.⁶⁹

The density was determined from NpT simulations in which the pressure was held constant by an Andersen's barostat⁷⁰ with a piston mass of $42.65 \cdot 10^6 \text{ kg m}^{-4}$. The system was first equilibrated with NVT boundary conditions for 50 000 time steps, followed by an NpT equilibration for 800 000 time steps. The length of the production phase of the NpT simulation run was 1 000 000 time steps.

The osmotic pressure Π was determined with the OPAS method,^{50–52} and then used for calculating the water activity a_W and the mean ionic activity coefficient γ_{AB}^{b*} . The OPAS method is described in detail in Ref. 50; it has already been applied successfully

to aqueous solutions containing the set of alkali and halide ions⁵¹ as well as to mixtures of molecular species.⁵² In the present work, it is applied to solutions with a multi-center ion, i.e., nitrate, for the first time. In the OPAS method, the osmotic pressure Π of an electrolyte solution is determined from a simulation scenario that introduces a virtual semipermeable membrane through which only water molecules can pass. An OPAS simulation run consists of two steps:⁵⁰ first, the volume of the cubic box is determined in a pseudo- NpT run in which a desired pressure in the compartment containing the pure solvent is prescribed. Then, the osmotic pressure Π is sampled in an NVT run with the box volume V obtained in the preceding pseudo- NpT run. The pseudo- NpT run consisted of an equilibration phase of 500 000 time steps followed by a production phase of 2 000 000 time steps. The NVT run consisted of an equilibration phase of 500 000 time steps followed by a production phase of 10 000 000 time steps, in which the osmotic pressure Π was sampled. For further information, the reader is referred to Kohns *et al.*⁵⁰

The self-diffusion coefficients and the radial distribution functions were calculated in the NVT ensemble. The box volume V and, hence, the density of the NVT simulation run were set according to a preceding NpT simulation run at the same temperature and composition. In the NVT simulation run, the system was first equilibrated for 200 000 time steps before sampling in the production phase for 2 400 000 time steps. The sampling length of the autocorrelation function for the Green–Kubo^{63,64} formalism was set to 10 000 MD steps and the result of every fifth time step was used for calculating the autocorrelation function. A time span of 200 time steps was introduced between the origins of two subsequent auto-correlation functions, so that in total 11 950 auto-correlation functions were sampled per simulation. The radial distribution function was determined and averaged every 10 000 time steps. The radial distribution function was calculated up to the cut-off radius of 15 Å and was divided into 500 equally sized bins.

III. RESULTS AND DISCUSSION

In the following, we compare the predictive simulation results with experimental data for each of the studied thermophysical and structural properties. For most properties, experimental data were only available at 298.15 K and 1 bar with the exception of density as well as the water activity of NaNO_3 solutions. Hence, almost all simulations were carried out at 298.15 K and 1 bar and, additionally, only some at 333.15 K and 1 bar.

The numerical simulation results are reported in the [supplementary material](#).

A. Reduced density

Figure 2 shows the reduced densities of all investigated nitrate salt solutions at 298.15 and 333.15 K. It is difficult to get reliable information on the solubility of molecular models of salt + solvent systems,^{14,15,49} and no corresponding effort was made here, especially as it is known that models that predict fluid properties of salt solutions well may give poor results for the solubility.⁴⁹ The kinetics of the solid formation from liquid solutions are slow and the simulation times that were used in the present study are too low to expect observing solid formation even when the salt concentration is above the solubility (which we do not know

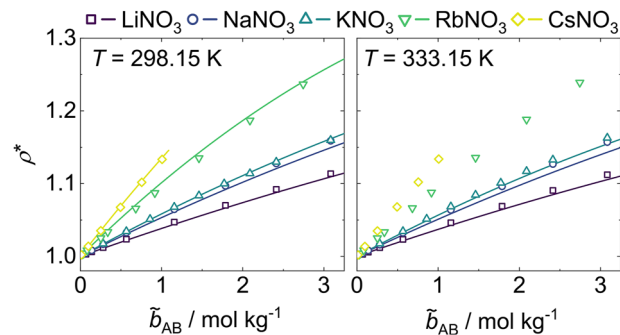


FIG. 2. Reduced density ρ^* as a function of the salt molality \tilde{b}_{AB} for aqueous solutions of the alkali nitrates LiNO_3 , NaNO_3 , KNO_3 , RbNO_3 , and CsNO_3 ; at 298.15 K and 333.15 K, 1 bar. Symbols show the simulation results, error bars are within symbol size. The solid lines represent correlations of experimental data from the Dortmund Data Bank⁵⁹ (for details, see the [supplementary material](#)). No experimental data were available for RbNO_3 and CsNO_3 at 333.15 K.

exactly). Despite this, we have limited the concentration range in which the simulation studies were carried out to a range in which the real solutions are still liquid: for LiNO_3 , NaNO_3 , KNO_3 , and RbNO_3 the maximal molality was 3 mol kg^{-1} , for CsNO_3 it was 1 mol kg^{-1} .

Figure 2 shows that for all studied solutions and both studied temperatures, the predicted density matches the experimental data well, the deviations are generally below 1%. Nevertheless, systematic trends of the deviations are observed for both temperatures: the density is slightly underestimated for LiNO_3 and NaNO_3 , while it is slightly overestimated for RbNO_3 and CsNO_3 , i.e., the deviations depend on the mass of the alkali cation. No comparison could be carried out for RbNO_3 and CsNO_3 at 333 K, as no experimental data were available, but we would expect the same trend as for 298 K. Considering the fact that no adjustments of parameters were made, the predictions for the density are excellent.

B. Water activity and mean ionic activity coefficients

Figure 3 shows the results for the water activity a_w and the mean ionic activity coefficient γ_{AB}^{b*} as a function of the overall molality \tilde{b}_{AB} at 298.15 K for all studied alkali nitrate salts. The simulation results are compared in Fig. 3 to correlations of experimental data taken from Hamer and Wu.⁶⁰ The numerical values of the fit parameters of the correlation to the simulation results [cf. Eqs. (11) and (13)] are given in Table III.

In contrast to the vast majority of strong electrolytes in an aqueous solution, the mean ionic activity coefficients of the alkali nitrates do not have a minimum as a function of concentration, with the exception of LiNO_3 . The molecular models predict this uncommon behavior well, however, they fail to predict the minimum for LiNO_3 . This deficiency regarding LiNO_3 is not surprising, since model parameters of Li^+ and Na^+ are very similar. Consequently, no strongly differing behavior in terms of the activity coefficient is to be expected for their nitrate salts. To investigate this more closely, we have conducted a parameter variation study for the Li^+ model, the results of which are reported in the [supplementary material](#). Regarding the

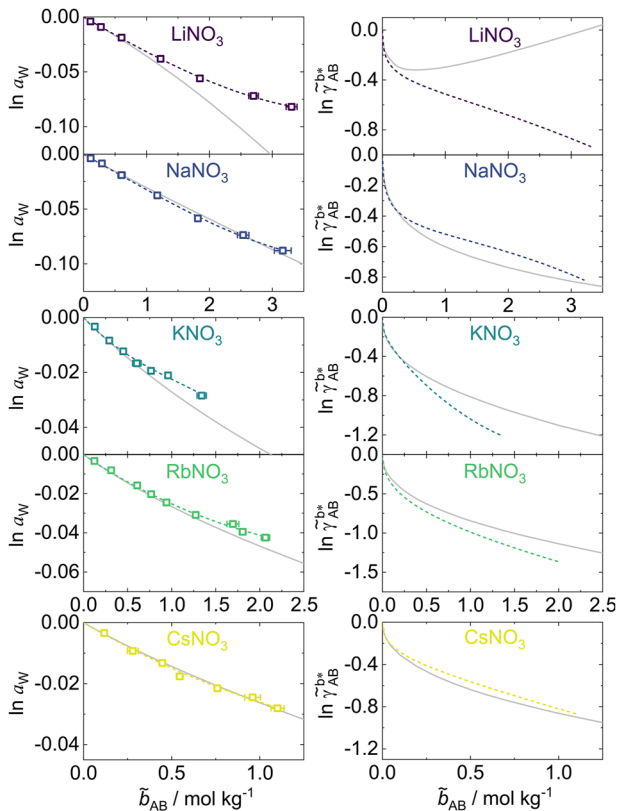


FIG. 3. Solvent activity a_w and mean ionic activity coefficients γ_{AB}^{b*} as a function of the salt molality \tilde{b}_{AB} for all investigated alkali nitrate salts at 298.15 K and 1 bar. Open squares show the simulation results for the solvent activity a_w . The dashed lines represent the correlations of the simulation data, from which also the mean ionic activity coefficients γ_{AB}^{b*} were calculated [cf. Eqs. (11) and (13)]. The gray solid lines represent correlations to experimental data taken from Hamer and Wu.⁶⁰

other nitrate salts, also quantitatively, the agreement between experiment and simulation is good, especially for solutions of NaNO₃, RbNO₃, and CsNO₃, considering that activities and related properties are very sensitive and difficult to predict by any other means. With increasing concentrations, it becomes increasingly difficult to

TABLE III. Summary of the parameters B , β , and C used in Eqs. (11) and (13) for fitting the solvent activity data obtained with the OPAS method for all alkali nitrate salts (cf. Fig. 3 and Fig. 4). All parameters are valid for 298.15 K, except for those in the last row. For the parameter A , cf. the discussion of Eq. (12).

Salt	B	β	C
LiNO ₃	2.2331	-0.0309	-0.0082
NaNO ₃	1.5871	0.0173	-0.0131
KNO ₃	3.8317	-0.4258	0.0976
RbNO ₃	0.8255	-0.1045	0.0009
CsNO ₃	2.5551	-0.1909	0.0019
NaNO ₃ (333.15 K)	1.2762	0.0386	-0.0117

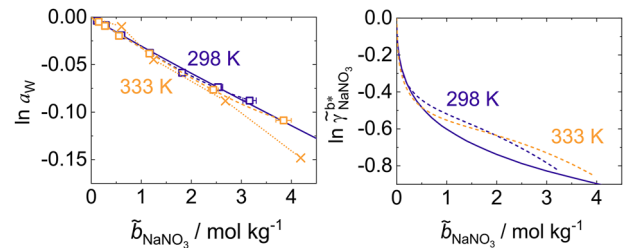


FIG. 4. Solvent activity a_w and mean ionic activity coefficient γ_{AB}^{b*} as a function of the salt molality \tilde{b}_{AB} for aqueous solutions of NaNO₃ at 298.15 and 333.15 K; both at 1 bar. Open squares show the simulation results for the solvent activity a_w . The dashed lines represent correlations of the simulation data, from which also the mean ionic activity coefficients γ_{AB}^{b*} were calculated [cf. Eqs. (11) and (13)]. The solid purple lines represent correlations to experimental data taken from Hamer and Wu⁶⁰ at 298.15 K. The orange crosses in the left panel represent points derived from the experimental vapor pressure data of Galleguillos *et al.*⁷¹ at 333.15 K; the dotted orange lines connect these individual points and are guides to the eye only.

correctly model the behavior of water activity and mean ionic activity coefficient for electrolyte solutions. Hence, the simulation results deviate increasingly from the experimental results for higher concentrations. This can be observed especially for LiNO₃ and KNO₃. Nonetheless, with the exception of LiNO₃, the water activity and the mean ionic activity coefficient are predicted well, especially at low concentrations.

Activity data at temperatures other than 298 K are scarce in the literature, even for important electrolytes such as alkali nitrates. Molecular simulations are an intriguing option to predict these properties. To further assess the predictive capabilities of the model set studied in this work, we studied the water activity and mean ionic activity coefficient of NaNO₃ solutions at 333 K. This system and temperature were chosen because experimental information on the water activity can be derived from the vapor pressure data by Galleguillos *et al.*,⁷¹ when assuming an ideal gas phase of pure water and using the vapor pressure of water of 0.199 bar at that temperature.⁷² The results of this study are shown in Fig. 4.

The experimental data show almost no temperature influence on the water activity in the studied temperature range up to a molality of about 2.5 mol kg⁻¹. The molecular simulations accurately predict this behavior. At higher concentrations, the experiments suggest that the water activity is lower at the higher temperature, which the molecular simulations do not capture. Nevertheless, especially for the lower concentrations the agreement is quite satisfactory considering that the molecular models are used in a strictly predictive manner.

C. Self-diffusion coefficients

The predictions of the self-diffusion coefficients of the potassium ion, the nitrate ion, and water in aqueous solutions of KNO₃ at 298.15 K and 1 bar are compared to experimental data in Fig. 5. To the best of our knowledge, this is the only alkali nitrate system for which experimental data are available in the literature. The self-diffusion coefficient at infinite dilution was determined in the present work from a linear fit. This self-diffusion coefficient

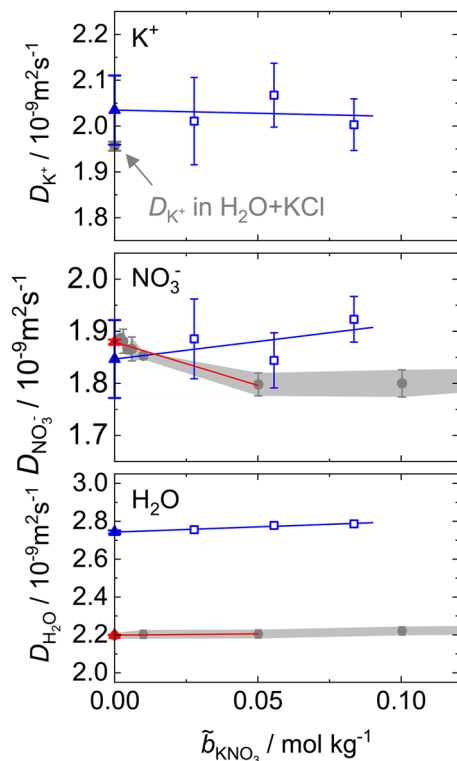


FIG. 5. Self-diffusion coefficients of K^+ , NO_3^- , and H_2O as a function of salt molality \tilde{b}_{KNO_3} for aqueous solutions of KNO_3 at 298.15 K and 1 bar. Open squares show the simulation results. Solid gray circles show experimental data from the literature (K^+ ,⁷³ NO_3^- ,⁷⁴ and H_2O ⁷⁵). For K^+ , the experimental self-diffusion coefficient at infinite dilution is given for the system $KCl + H_2O$, due to the lack of data for the system $KNO_3 + H_2O$. The areas shaded in light gray are guides to the eye indicating the range of experimental data including uncertainties. The filled triangles represent the self-diffusion coefficient at infinite dilution, which is extrapolated linearly (red line: experimental data, blue line: simulation results).

at infinite dilution is of particular interest due to the fact that the influence of the counter ion is negligible. Furthermore, at infinite dilution, the self-diffusion coefficient corresponds to the mutual transport diffusion coefficient of the ion.

The simulation result for the self-diffusion coefficient of the nitrate ion is in good agreement with the experimental value, which is only slightly overestimated. In contrast to the experimental trends, the simulation results suggest a slight increase in the self-diffusion coefficient of the nitrate ion with increasing concentration. However, there are considerable uncertainties of the simulation results, which arise from the extremely low concentrations studied, meaning that few ions are present in the simulation box despite large systems containing 16 000 particles that were studied. Hence, this finding should not be overinterpreted.

For the potassium ion a comparison to experimental data is only feasible for the infinite dilution due to the lack of experimental data on KNO_3 . Again, good agreement between the prediction from the simulation and the experimental data is observed, which, again, is only slightly overestimated.

The results from the present work confirm previous findings from the literature⁷⁶ that the self-diffusion coefficients of water at 298 K are overestimated by the SPC/E model by about 25%. This translates directly to the results for the electrolyte solutions. However, the slight increase in the self-diffusion coefficient of water upon adding KNO_3 is correctly predicted. As first pointed out in a study by Kim *et al.*⁷⁷ and summarized in recent reviews by Panagiotopoulos¹⁵ and Panagiotopoulos and Yue,⁷⁸ many non-polarizable models fail at predicting this trend correctly, but the present model combination for aqueous KNO_3 solutions does.

In summary, the self-diffusion coefficients of the ion models, especially of the NO_3^- ion, at high to infinite dilution are in good agreement with the experimental data. The infinite dilution of NO_3^- ions is of particular interest since it is similar in all aqueous solutions of the alkali nitrate model set. For more information as well as numerical results of the self-diffusion coefficients at infinite dilution, see the [supplementary material](#).

D. Radial distribution functions

Figure 6 shows the radial distribution functions of different interaction sites in an aqueous solution of $NaNO_3$ with a molality of $3.084 \text{ mol kg}^{-1}$ at 298.15 K and 1 bar. For this system, experimental data are available in the literature for the positions of the first maxima $r_{\text{max}1}$ of the radial distribution functions. To the best of our knowledge, this is the only alkali nitrate system for which such a comparison can be carried out due to a lack of experimental data for other systems. The molality of the experimental data from Kameda *et al.*^{79,80} is at $6.168 \text{ mol kg}^{-1}$ and Megyes *et al.*³² report data in a range from 2 to 10 mol kg^{-1} . The influence of the concentration on the position of the first maximum is negligible as shown in the work of Megyes *et al.*³²

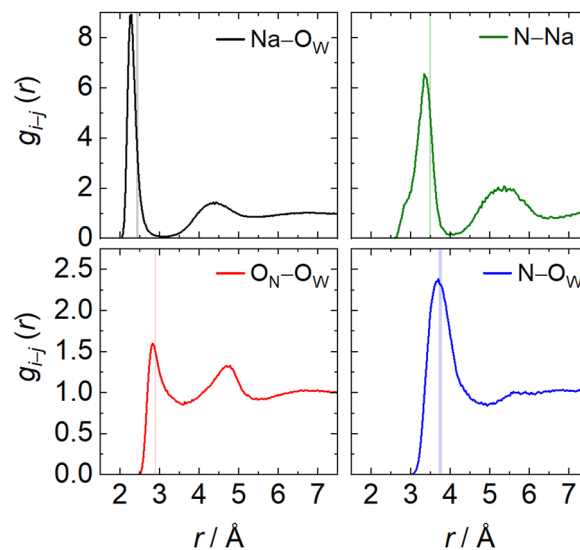


FIG. 6. Radial distribution functions of different interaction sites in a $NaNO_3$ solution with a molality of $3.084 \text{ mol kg}^{-1}$ at 298.15 K and 1 bar. Solid lines show the simulation results. Experimental data for the position of the first maximum $r_{\text{max}1}$ from the literature (g_{Na-O_w} ,³² $g_{O_N-O_w}$,⁸⁰ g_{N-Na} ,³² g_{N-O_w} ^{79,80}) are given by the shaded vertical bars including statistical uncertainties.

Overall, the favorable agreement is observed between the experimental data for the locations of the first maxima of the different radial distribution functions and the predictions from the molecular simulations. The predictions of the positions of the first maximum in the O_N-O_W RDF and the $N-O_W$ RDF are almost within the narrow uncertainty of the experimental results. This indicates that the structure of water around the NO_3^- ion is represented very well by the model. The results for the Na^+ ion are less accurate: the position of the first maximum of the Na^+-O_W RDF and the $N-Na^+$ RDF is predicted too low. This is not unexpected, as RDF involving the Na^+ ion model and SPC/E water have shown similar trends in simulations of aqueous alkali halide systems.¹⁷

A further analysis of the radial distribution functions from molecular simulation reveals two intriguing aspects. First, comparing g_{N-Na} and g_{N-O_W} shows that the Na^+ cations get somewhat more closely to the nitrogen atom of the nitrate anion than water molecules do. This is a quite surprising finding since both Na^+ and the nitrogen interaction site have positive point charges. Second, there is a shoulder in g_{N-Na} at about $r = 2.9$ Å. The position of this shoulder in g_{N-Na} matches the unlike LJ size parameter of the $N-Na^+$ interaction, which is also 2.9 Å. Hence, a small number of Na^+ ions coordinate closer to the nitrogen atom of the nitrate anion in that distance, while the majority of the Na^+ ions are found at around 3.34 Å in the first maximum.

Both peculiarities can be explained by the fact that the positively charged nitrogen atom on the nitrate anion is surrounded by three negatively charged oxygen atoms, which strongly attract the Na^+ ions and shield the positive charge on the nitrogen. In addition, the overall net charge of the nitrate anion is negative, which makes it attractive for Na^+ . Finally, the size parameter of the employed Na^+ model is about 40% smaller than that of the SPC/E water model, so it has a simple geometric advantage in the competition for the spots closest to the nitrate anion.

In summary, the structure in short range around all investigated interaction sites is well predicted, especially for the NO_3^- ion, which is the main focus of this work.

IV. CONCLUSIONS

In this work, a set of molecular models for alkali nitrate salts in an aqueous solution is proposed. This set is used for predicting the thermophysical and structural properties of the aqueous nitrate salt solutions and the results are compared to experimental data. Furthermore, the water activity and the mean ionic activity coefficients are predicted in this study in a broad concentration range by molecular simulations for these five alkali nitrates. The models for the individual species — cations, nitrate, and water — were developed independently of each other by different groups and are deployed in a strictly predictive manner using the Lorentz–Berthelot rules. The alkali cation models were developed for the use in conjunction with halide ions and the SPC/E water model. The nitrate model on the other hand has been derived on the basis of quantum mechanical calculations and developed for usage with a water model developed by the original authors. Especially, the predictions for the density and the radial distribution functions are in good agreement with the available experimental data. The water activity and the mean ionic activity coefficients of the alkali nitrate solutions are in remarkable

agreement with experimental data, the only exception being solutions of $LiNO_3$. The self-diffusion coefficients are also predicted well with the exception of water, which is an inherent issue of the SPC/E water model.

Overall, the good agreement of all investigated properties with experimental data is surprising, considering the fact that the molecular models for the nitrate anion, and the cations were developed independently by different authors, and no cross-interactions were adjusted. The presented set of molecular models is a promising tool to further investigate the influence of mixtures of different alkali nitrate salts or mixtures of alkali nitrate and halide salts on thermophysical properties of the aqueous solution, since set is part of a consistent model family that has provided good predictions for single salt mixtures.

SUPPLEMENTARY MATERIAL

The [supplementary material](#) contains details on the procedure and parameters of the polynomial fit to the experimental density data for all considered nitrate salts. Moreover, the [supplementary material](#) contains an OPAS simulation study in which the LJ parameters of the Li^+ cation model were varied in aqueous solutions of $LiNO_3$. Additionally, details on the determination of the standard error for the extrapolated self-diffusion coefficients at infinite dilution and compilations of the numerical values of the simulation results considered in this work are given in the [supplementary material](#).

ACKNOWLEDGMENTS

The present work was conducted under the auspices of the Boltzmann-Zuse Society of Computational Molecular Engineering (BZS), and the simulations were carried out on the Regional University Computing Center Kaiserslautern (RHRK) under the grant TUK-MTD, the High Performance Computing Center Stuttgart (HLRS) under the Grant No. MMHBF2, as well as the Leibniz Supercomputing Centre (LRZ) under the Grant No. (AMSEL)² (pn56mo). We thank Yannik Sinnwell for his assistance in carrying out molecular simulations.

AUTHOR DECLARATIONS

Conflict of Interest

The authors have no conflicts to disclose.

Author Contributions

Dominik Schaefer: Conceptualization (equal); Data curation (equal); Formal analysis (equal); Investigation (equal); Methodology (equal); Software (lead); Validation (lead); Visualization (lead); Writing – original draft (equal); Writing – review & editing (equal). **Maximilian Kohns:** Conceptualization (equal); Formal analysis (equal); Funding acquisition (equal); Investigation (equal); Methodology (equal); Project administration (lead); Resources (equal);

Supervision (lead); Validation (equal); Visualization (equal); Writing – original draft (equal); Writing – review & editing (equal). **Hans Hasse**: Conceptualization (equal); Formal analysis (equal); Funding acquisition (equal); Investigation (equal); Methodology (equal); Project administration (equal); Supervision (lead); Writing – original draft (equal); Writing – review & editing (lead).

DATA AVAILABILITY

The data that support the findings of this study are available within the article and its [supplementary material](#).

REFERENCES

- 1 K. S. Pitzer, “Thermodynamics of electrolytes. I. Theoretical basis and general equations,” *J. Phys. Chem.* **77**, 268–277 (1973).
- 2 K. S. Pitzer and J. J. Kim, “Thermodynamics of electrolytes. IV. Activity and osmotic coefficients for mixed electrolytes,” *J. Am. Chem. Soc.* **96**, 5701–5707 (1974).
- 3 T. J. Edwards, G. Maurer, J. Newman, and J. M. Prausnitz, “Vapor-liquid equilibria in multicomponent aqueous solutions of volatile weak electrolytes,” *AIChE J.* **24**, 966–976 (1978).
- 4 C.-C. Chen, H. I. Britt, J. F. Boston, and L. B. Evans, “Extension and application of the Pitzer equation for vapor-liquid equilibrium of aqueous electrolyte systems with molecular solutes,” *AIChE J.* **25**, 820–831 (1979).
- 5 P. de Alcântara Pessôa Filho and G. Maurer, “An extension of the Pitzer equation for the excess Gibbs energy of aqueous electrolyte systems to aqueous polyelectrolyte solutions,” *Fluid Phase Equilib.* **269**, 25–35 (2008).
- 6 C.-C. Chen and L. B. Evans, “A local composition model for the excess Gibbs energy of aqueous electrolyte systems,” *AIChE J.* **32**, 444–454 (1986).
- 7 P. Debye and E. Hückel, “Zur Theorie der Elektrolyte,” *Phys. Z.* **24**, 185–206 (1923).
- 8 C. Held, L. F. Cameretti, and G. Sadowski, “Modeling aqueous electrolyte solutions: Part I. Fully dissociated electrolytes,” *Fluid Phase Equilib.* **270**, 87–96 (2008).
- 9 C. Held, T. Reschke, S. Mohammad, A. Luza, and G. Sadowski, “ePC-SAFT revised,” *Chem. Eng. Res. Des.* **92**, 2884–2897 (2014).
- 10 A. Schlaikjer, K. Thomsen, and G. M. Kontogeorgis, “eCPA: An ion-specific approach to parametrization,” *Fluid Phase Equilib.* **470**, 176–187 (2018).
- 11 M. D. Olsen, G. M. Kontogeorgis, X. Liang, and N. von Solms, “Investigation of the performance of e-CPA for a wide range of properties for aqueous NaCl solutions,” *Fluid Phase Equilib.* **548**, 113167 (2021).
- 12 M. Kohns, G. Lazarou, S. Kournopoulos, E. Forte, F. A. Perdomo, G. Jackson, C. S. Adjiman, and A. Galindo, “Predictive models for the phase behaviour and solution properties of weak electrolytes: Nitric, sulphuric, and carbonic acids,” *Phys. Chem. Chem. Phys.* **22**, 15248–15269 (2020).
- 13 A. J. Haslam, A. González-Pérez, S. Di Lecce, S. H. Khalit, F. A. Perdomo, S. Kournopoulos, M. Kohns, T. Lindeboom, M. Wehbe, S. Febra, G. Jackson, C. S. Adjiman, and A. Galindo, “Expanding the applications of the SAFT- γ Mie group-contribution equation of state: Prediction of thermodynamic properties and phase behavior of mixtures,” *J. Chem. Eng. Data* **65**, 5862–5890 (2020).
- 14 W. R. Smith, I. Nezbeda, J. Kolafa, and F. Moučka, “Recent progress in the molecular simulation of thermodynamic properties of aqueous electrolyte solutions,” *Fluid Phase Equilib.* **466**, 19–30 (2018).
- 15 A. Z. Panagiotopoulos, “Simulations of activities, solubilities, transport properties, and nucleation rates for aqueous electrolyte solutions,” *J. Chem. Phys.* **153**, 010903 (2020).
- 16 S. Deublein, J. Vrabec, and H. Hasse, “A set of molecular models for alkali and halide ions in aqueous solution,” *J. Chem. Phys.* **136**, 084501 (2012).
- 17 S. Reiser, S. Deublein, J. Vrabec, and H. Hasse, “Molecular dispersion energy parameters for alkali and halide ions in aqueous solution,” *J. Chem. Phys.* **140**, 044504 (2014).
- 18 H. J. C. Berendsen, J. R. Grigera, and T. P. Straatsma, “The missing term in effective pair potentials,” *J. Phys. Chem.* **91**, 6269–6271 (1987).
- 19 B. Elvers, *Ullmann’s Encyclopedia of Industrial Chemistry* (Wiley, 2000).
- 20 W. L. Jorgensen, J. Chandrasekhar, J. D. Madura, R. W. Impey, and M. L. Klein, “Comparison of simple potential functions for simulating liquid water,” *J. Chem. Phys.* **79**, 926–935 (1983).
- 21 H. J. C. Berendsen, J. P. M. Postma, W. F. van Gunsteren, and J. Hermans, “Interaction models for water in relation to protein hydration,” in *Intermolecular Forces*, The Jerusalem Symposia on Quantum Chemistry and Biochemistry (Springer Netherlands, 1981), pp. 331–342, see https://link.springer.com/chapter/10.1007/978-94-015-7658-1_21.
- 22 S. Izadi, R. Anandakrishnan, and A. V. Onufriev, “Building water models: A different approach,” *J. Phys. Chem. Lett.* **5**, 3863–3871 (2014).
- 23 V. Vchirawongkwin, H. Sato, and S. Sakaki, “RISM-SCF-SEDD study on the symmetry breaking of carbonate and nitrate anions in aqueous solution,” *J. Phys. Chem. B* **114**, 10513–10519 (2010).
- 24 V. Vchirawongkwin, C. Kritayakornupong, A. Tongraar, and B. M. Rode, “Symmetry breaking and hydration structure of carbonate and nitrate in aqueous solutions: A study by ab initio quantum mechanical charge field molecular dynamics,” *J. Phys. Chem. B* **115**, 12527–12536 (2011).
- 25 J. Thøgersen, J. Réhault, M. Odelius, T. Ogden, N. K. Jena, S. J. K. Jensen, S. R. Keiding, and J. Helbing, “Hydration dynamics of aqueous nitrate,” *J. Phys. Chem. B* **117**, 3376–3388 (2013).
- 26 S. Matsunaga, “Molecular simulation study of structure and dynamical properties of nitrate anion in sodium chloride aqueous solution,” *Mol. Simul.* **41**, 913–917 (2014).
- 27 P. Banerjee, S. Yashonath, and B. Bagchi, “Coupled jump rotational dynamics in aqueous nitrate solutions,” *J. Chem. Phys.* **145**, 234502 (2016).
- 28 A. Laaksonen and H. Kovacs, “Silver nitrate in aqueous solution and as molten salt: A molecular dynamics simulation and NMR relaxation study,” *Can. J. Chem.* **72**, 2278–2285 (1994).
- 29 G.-w. Lu, Y.-f. Li, W. Sun, and C.-x. Li, “Molecular dynamics simulation of hydration structure of KNO₃ electrolyte solution,” *Chin. J. Chem. Phys.* **20**, 22–30 (2007).
- 30 H. Krienke and G. Schmeer, “Hydration of molecular anions with oxygen sites—A Monte Carlo study,” *Z. Phys. Chem.* **218**, 749–764 (2004).
- 31 H. Krienke and D. Opalka, “Hydration of molecular ions: A molecular dynamics study with a SPC/E water model,” *J. Phys. Chem. C* **111**, 15935–15941 (2007).
- 32 T. Megyes, S. Bálint, E. Peter, T. Grósz, I. Bakó, H. Krienke, and M.-C. Bellissent-Funel, “Solution structure of NaNO₃ in water: Diffraction and molecular dynamics simulation study,” *J. Phys. Chem. B* **113**, 4054–4064 (2009).
- 33 H. Krienke, “On the influence of molecular structure on the conductivity of electrolyte solutions—Sodium nitrate in water,” *Condens. Matter Phys.* **16**, 43006 (2013).
- 34 S. Jayaraman, A. P. Thompson, O. A. von Lilienfeld, and E. J. Maginn, “Molecular simulation of the thermal and transport properties of three alkali nitrate salts,” *Ind. Eng. Chem. Res.* **49**, 559–571 (2009).
- 35 W. J. Xie, Z. Zhang, and Y. Q. Gao, “Ion pairing in alkali nitrate electrolyte solutions,” *J. Phys. Chem. B* **120**, 2343–2351 (2016).
- 36 L. X. Dang, T.-M. Chang, M. Roeselova, B. C. Garrett, and D. J. Tobias, “On NO₃⁻-H₂O interactions in aqueous solutions and at interfaces,” *J. Chem. Phys.* **124**, 066101 (2006).
- 37 B. Minofar, R. Vácha, A. Wahab, S. Mahiuddin, W. Kunz, and P. Jungwirth, “Propensity for the air/water interface and ion pairing in magnesium acetate vs magnesium nitrate solutions: Molecular dynamics simulations and surface tension measurements,” *J. Phys. Chem. B* **110**, 15939–15944 (2006).
- 38 P. Salvador, J. E. Curtis, D. J. Tobias, and P. Jungwirth, “Polarizability of the nitrate anion and its solvation at the air/water interface,” *Phys. Chem. Chem. Phys.* **5**, 3752–3757 (2003).
- 39 J. L. Thomas, M. Roeselová, L. X. Dang, and D. J. Tobias, “Molecular dynamics simulations of the solution–air interface of aqueous sodium nitrate,” *J. Phys. Chem. A* **111**, 3091–3098 (2007).
- 40 G.-w. Lu, C.-x. Li, W.-c. Wang, and Z.-h. Wang, “Structure of KNO₃ electrolyte solutions: A Monte Carlo study,” *Fluid Phase Equilib.* **225**, 1–11 (2004).

- ⁴¹G.-w. Lu, C.-x. Li, W.-c. Wang, and Z.-h. Wang, "A Monte Carlo simulation on structure and thermodynamics of potassium nitrate electrolyte solution," *Mol. Phys.* **103**, 599–610 (2005).
- ⁴²M. C. G. Lebrero, D. E. Bikiel, M. D. Elola, D. A. Estrin, and A. E. Roitberg, "Solvent-induced symmetry breaking of nitrate ion in aqueous clusters: A quantum-classical simulation study," *J. Chem. Phys.* **117**, 2718–2725 (2002).
- ⁴³S. W. Rick, S. J. Stuart, and B. J. Berne, "Dynamical fluctuating charge force fields: Application to liquid water," *J. Chem. Phys.* **101**, 6141–6156 (1994).
- ⁴⁴F. Moučka, M. Lísal, J. Škvor, J. Jirsák, I. Nezbeda, and W. R. Smith, "Molecular simulation of aqueous electrolyte solubility. 2. Osmotic ensemble Monte Carlo methodology for free energy and solubility calculations and application to NaCl," *J. Phys. Chem. B* **115**, 7849–7861 (2011).
- ⁴⁵F. Moučka, I. Nezbeda, and W. R. Smith, "Molecular simulation of aqueous electrolytes: Water chemical potential results and Gibbs-Duhem equation consistency tests," *J. Chem. Phys.* **139**, 124505 (2013).
- ⁴⁶F. Moučka, I. Nezbeda, and W. R. Smith, Chemical Ehara, "Theoretical Prediction by polarizable force fields," *J. Chem. Theory Comput.* **11**, 1756–1764 (2015).
- ⁴⁷M. Lísal, W. R. Smith, and J. Kolafa, "Molecular simulations of aqueous electrolyte solubility: 1. The expanded-ensemble osmotic molecular dynamics method for the solution phase," *J. Phys. Chem. B* **109**, 12956–12965 (2005).
- ⁴⁸Z. Mester and A. Z. Panagiotopoulos, "Mean ionic activity coefficients in aqueous NaCl solutions from molecular dynamics simulations," *J. Chem. Phys.* **142**, 044507 (2015).
- ⁴⁹Z. Mester and A. Z. Panagiotopoulos, "Temperature-dependent solubilities and mean ionic activity coefficients of alkali halides in water from molecular dynamics simulations," *J. Chem. Phys.* **143**, 044505 (2015).
- ⁵⁰M. Kohns, S. Reiser, M. Horsch, and H. Hasse, "Solvent activity in electrolyte solutions from molecular simulation of the osmotic pressure," *J. Chem. Phys.* **144**, 084112 (2016).
- ⁵¹M. Kohns, M. Schappals, M. Horsch, and H. Hasse, "Activities in aqueous solutions of the alkali halide salts from molecular simulation," *J. Chem. Eng. Data* **61**, 4068–4076 (2016).
- ⁵²M. Kohns, M. Horsch, and H. Hasse, "Activity coefficients from molecular simulations using the OPAS method," *J. Chem. Phys.* **147**, 144108 (2017).
- ⁵³H. A. Lorentz, "Ueber die Anwendung des Satzes vom Virial in der Kinetischen Theorie der Gase," *Ann. Phys.* **248**, 127–136 (1881).
- ⁵⁴D. Berthelot, "Sur le mélange des gaz," *C. R. Acad. Sci.* **126**, 1703–1706 (1898).
- ⁵⁵S. Reiser, M. Horsch, and H. Hasse, "Temperature dependence of the density of aqueous alkali halide salt solutions by experiment and molecular simulation," *J. Chem. Eng. Data* **59**, 3434–3448 (2014).
- ⁵⁶S. Deublein, S. Reiser, J. Vrabec, and H. Hasse, "A set of molecular models for alkaline-earth cations in aqueous solution," *J. Phys. Chem. B* **116**, 5448–5457 (2012).
- ⁵⁷D. Saric, M. Kohns, and J. Vrabec, "Dielectric constant and density of aqueous alkali halide solutions by molecular dynamics: A force field assessment," *J. Chem. Phys.* **152**, 164502 (2020).
- ⁵⁸W. Wagner and A. Pruß, "The IAPWS formulation 1995 for the thermodynamic properties of ordinary water substance for general and scientific use," *J. Phys. Chem. Ref. Data* **31**, 387–535 (2002).
- ⁵⁹Dortmund Data Bank, www.ddbst.com, 2022.
- ⁶⁰W. J. Hamer and Y. C. Wu, "Osmotic coefficients and mean activity coefficients of uni-univalent electrolytes in water at 25 °C," *J. Phys. Chem. Ref. Data* **1**, 1047–1100 (1972).
- ⁶¹R. Fingerhut, G. Guevara-Carrion, I. Nitzke, D. Saric, J. Marx, K. Langenbach, S. Prokopen, D. Celný, M. Bernreuther, S. Stephan, M. Kohns, H. Hasse, and J. Vrabec, "ms2: A molecular simulation tool for thermodynamic properties, release 4.0," *Comput. Phys. Commun.* **262**, 107860 (2021).
- ⁶²R. Fuentes-Azcatl, N. Mendoza, and J. Alejandro, "Improved SPC force field of water based on the dielectric constant: SPC/ε," *Physica A* **420**, 116–123 (2015).
- ⁶³M. S. Green, "Markoff random processes and the statistical mechanics of time-dependent phenomena. II. Irreversible processes in fluids," *J. Chem. Phys.* **22**, 398–413 (1954).
- ⁶⁴R. Kubo, "Statistical-mechanical theory of irreversible processes. I. General theory and simple applications to magnetic and conduction problems," *J. Phys. Soc. Jpn.* **12**, 570–586 (1957).
- ⁶⁵G. A. Fernández, J. Vrabec, and H. Hasse, "Self diffusion and binary Maxwell–Stefan diffusion in simple fluids with the Green–Kubo method," *Int. J. Thermophys.* **25**, 175–186 (2004).
- ⁶⁶M. P. Allen and D. J. Tildesley, *Computer Simulation of Liquids* (Oxford University Press, 2017).
- ⁶⁷C. W. Gear, "The numerical integration of ordinary differential equations of various orders," Technical Report No. #ANL-7126, Argonne National Laboratory, IL, 1966, see https://www.researchgate.net/publication/24363098_The_Numerical_Integration_of_Ordinary_Differential_Equations_of_Various_Orders.
- ⁶⁸P. P. Ewald, "Die Berechnung optischer und elektrostatischer Gitterpotentiale," *Ann. Phys.* **369**, 253–287 (1921).
- ⁶⁹H. Flyvbjerg and H. G. Petersen, "Error estimates on averages of correlated data," *J. Chem. Phys.* **91**, 461–466 (1989).
- ⁷⁰H. C. Andersen, "Molecular dynamics simulations at constant pressure and/or temperature," *J. Chem. Phys.* **72**, 2384–2393 (1980).
- ⁷¹H. Galleguillos, D. Salavera, P. Vargas, and A. Coronas, "Experimental determination and prediction of the vapor pressure of some binary and quaternary aqueous solutions of alkaline nitrites and nitrates," *Fluid Phase Equilib.* **291**, 208–211 (2010).
- ⁷²E. W. Lemmon, I. Bell, M. L. Huber, and M. O. McLinden, "NIST standard reference database 23: Reference fluid thermodynamic and transport properties—REFPROP, version 10.0," *Standard Reference Data Program*, Gaithersburg (2018).
- ⁷³R. Mills and V. M. M. Lobo, *Self-Diffusion in Electrolyte Solutions* (Elsevier, 1989).
- ⁷⁴T. Hashitani and K. Tanaka, "Measurements of self-diffusion coefficients of the nitrate ion in aqueous solutions of potassium nitrate and calcium nitrate," *J. Chem. Soc., Faraday Trans. 1* **79**, 1765–1768 (1983).
- ⁷⁵K. Tanaka, "Measurements of self-diffusion coefficients of water in pure water and in aqueous electrolyte solutions," *J. Chem. Soc., Faraday Trans. 1* **71**, 1127–1131 (1975).
- ⁷⁶I. N. Tsimpanogiannis, O. A. Moutos, L. F. M. Franco, M. B. d. M. Spera, M. Erdős, and I. G. Economou, "Self-diffusion coefficient of bulk and confined water: A critical review of classical molecular simulation studies," *Mol. Simul.* **45**, 425–453 (2018).
- ⁷⁷J. S. Kim, Z. Wu, A. R. Morrow, A. Yethiraj, and A. Yethiraj, "Self-diffusion and viscosity in electrolyte solutions," *J. Phys. Chem. B* **116**, 12007–12013 (2012).
- ⁷⁸A. Z. Panagiotopoulos and S. Yue, "Dynamics of aqueous electrolyte solutions: Challenges for simulations," *J. Phys. Chem. B* **127**, 430–437 (2023).
- ⁷⁹Y. Kameda, H. Saitoh, and O. Uemura, "The hydration structure of NO₃⁻ in concentrated aqueous sodium nitrate solutions," *Bull. Chem. Soc. Jpn.* **66**, 1919–1923 (1993).
- ⁸⁰Y. Kameda, K. Sugawara, T. Usuki, and O. Uemura, "Hydration structure of Na⁺ in concentrated aqueous solutions," *Bull. Chem. Soc. Jpn.* **71**, 2769–2776 (1998).